Supporting Information

Achieving high ionic conductivity of LATP solid electrolyte via LiTFSI-assisted cold sintering process

Shanshan Yi,[a]† Shuyu Zhou,[a,b]† Yudong Liu,[a] PengPeng Dai,[a] Yuxin Liu,[a] Shixi Zhao*[a] and Guozhong Cao*[c]

[a.] *Shenzhen International Graduate School, Tsinghua University, Shenzhen, 518055, China.*

[b.] *School of Materials Science and Engineering, Tsinghua University, Beijing, 100084, China.*

[c.] *Department of Materials Science and Engineering, University of Washington, Seattle, WA 98195 (USA).*

† Shanshan Yi and Shuyu Zhou contributed equally to this work.

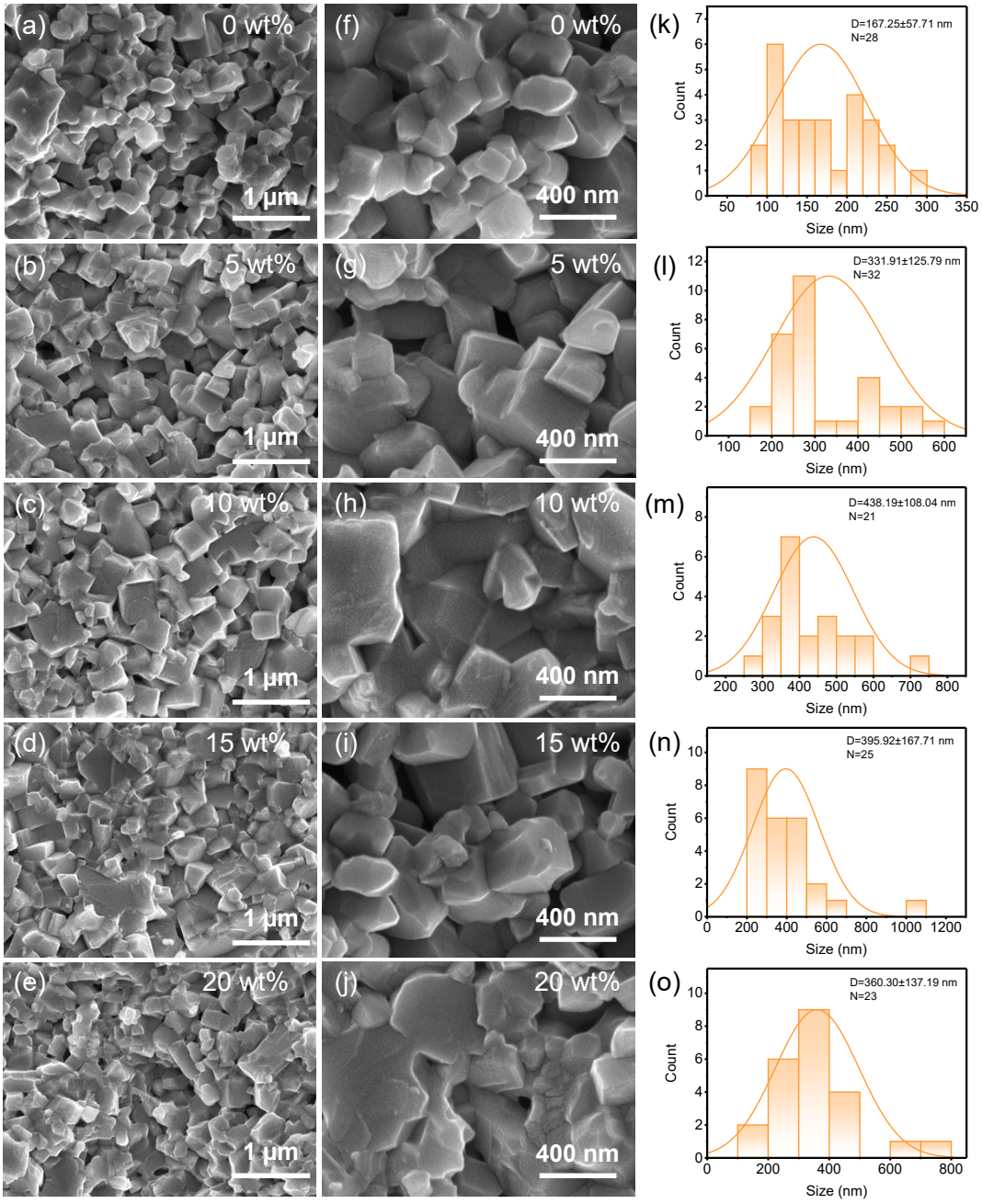

Fig. S1. SEM image and grain size distribution of CSH-LATP-xLiTFSI(650). (a,f,k): x=0; (b,g,l): x=0.05; (c,h,m): x=0.1; (d,i,n): x=0.15; (e,j,o): x=0.2.

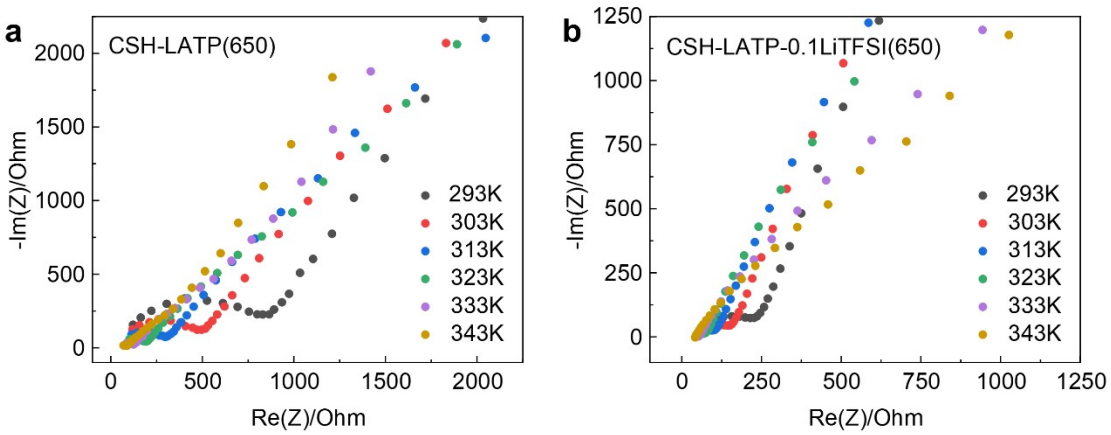

Fig. S2 EIS results of (a) CSH-LATP(650) and (b) CSH-LATP-0.1LiTFSI(650) at different temperature.

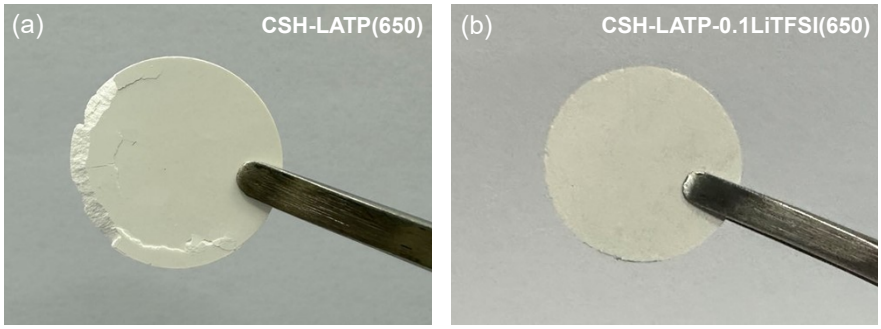

Fig. S3 digital images of (a) CSH-LATP(650) and (b) CSH-LATP-0.1LiTFSI(650).

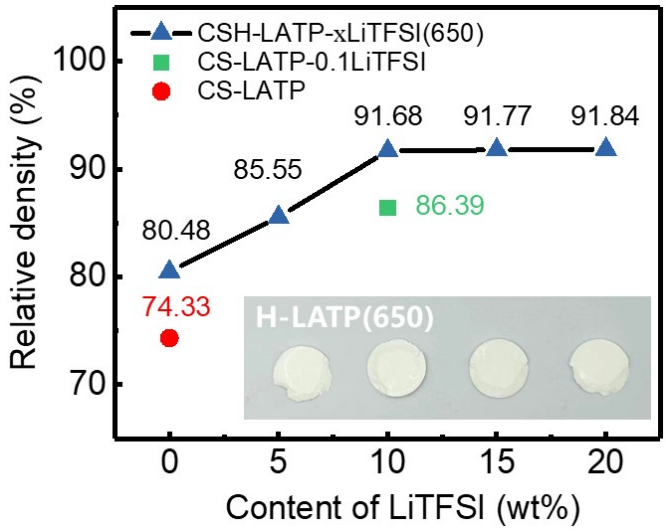

Fig. S4 Relative density of LATP pellets at different experiment condition and the digital images of H-LATP(650) at bottom right.

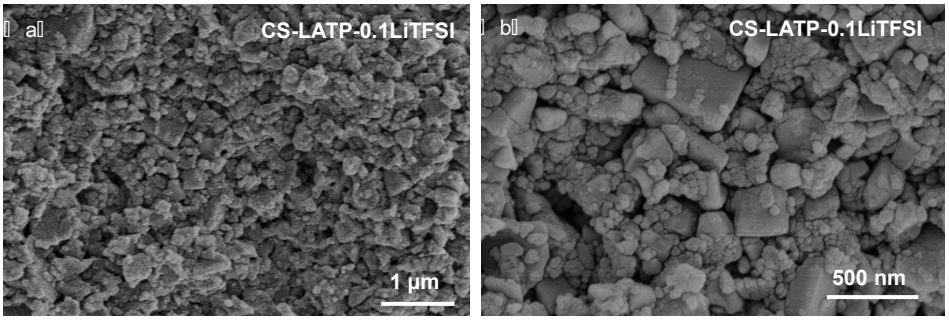

Figure S5 The SEM images of the cross section of CS-LATP-0.1LiTFSI.

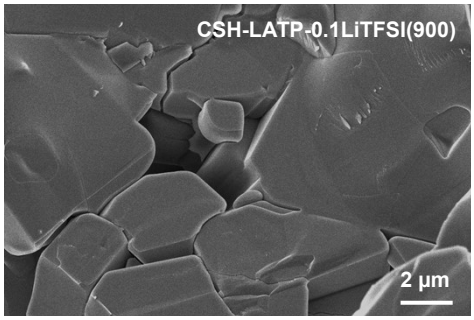

Fig. S6 The SEM images of the cross section of CSH-LATP-0.1LiTFSI(900).

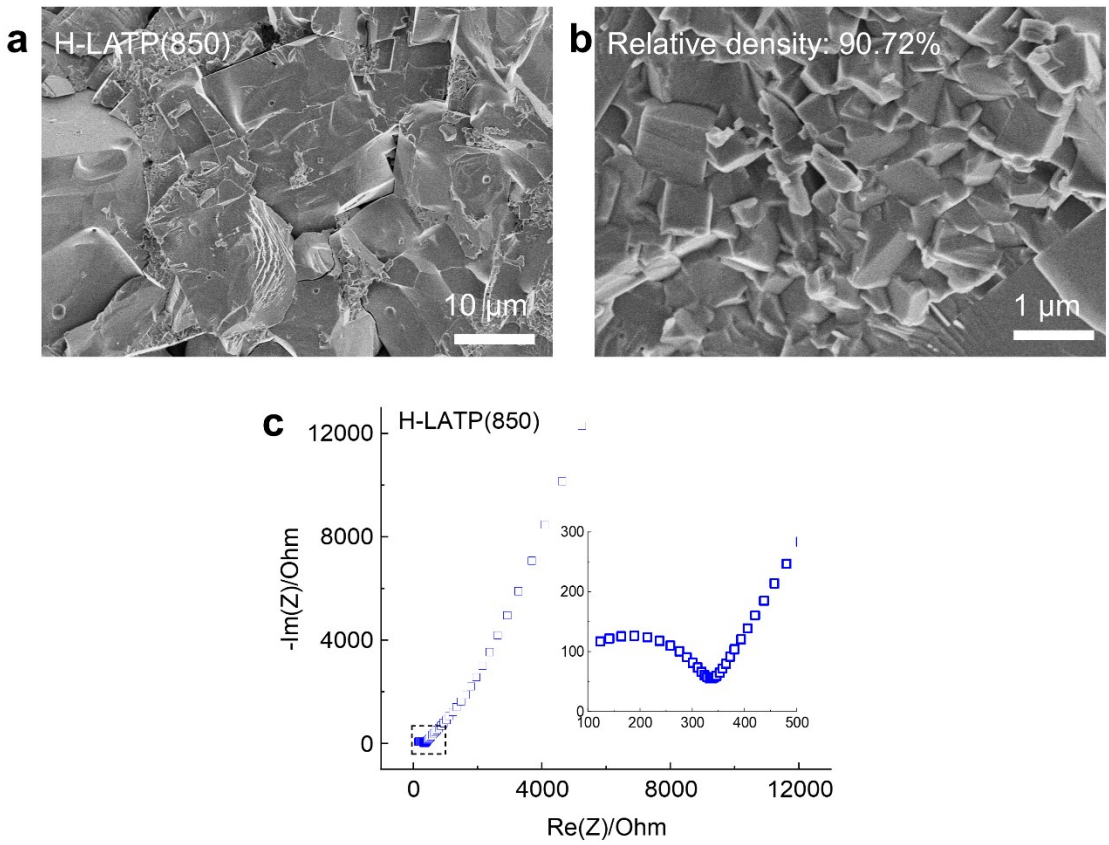

Fig. S7 (a,b) The SEM images of the cross section of H-LATP(850). (c) EIS results of H-LATP(850) at room temperature.

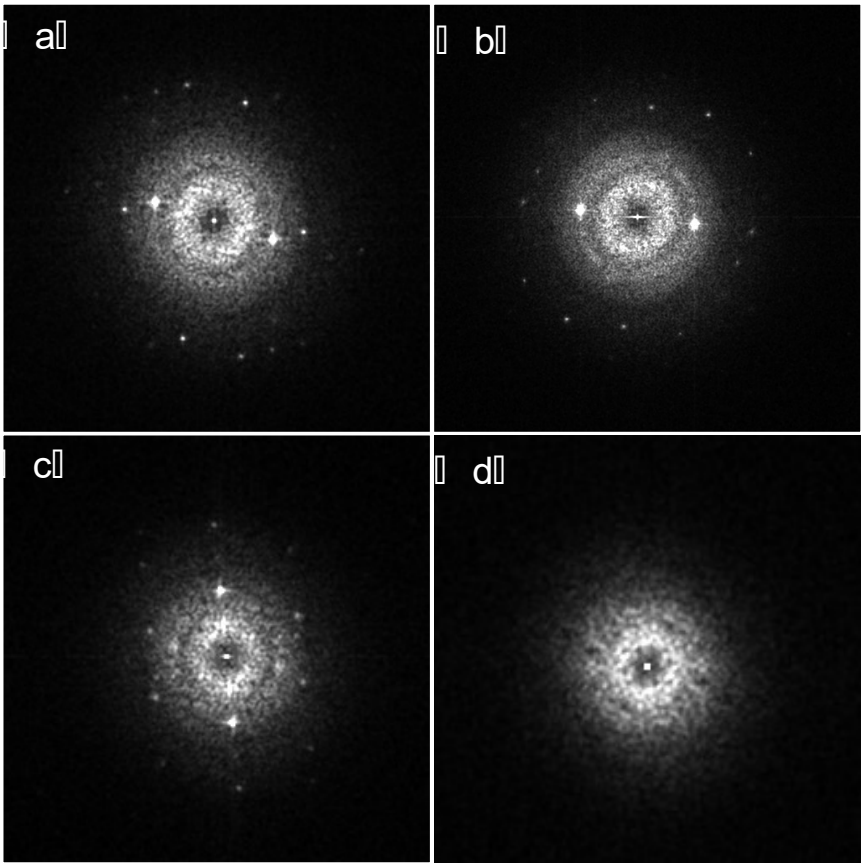

Fig. S8 Electron diffraction pattern of (a) area A, (b) area B, (c) area C and (d) area D of Fig. 4a.

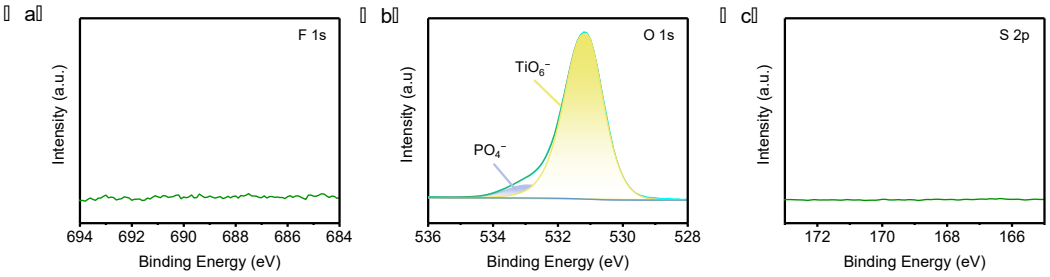

Fig. S9 XPS spectra of CSH-LATP(650): (a) F 1s; (b) O 1s; (c) S 2p.

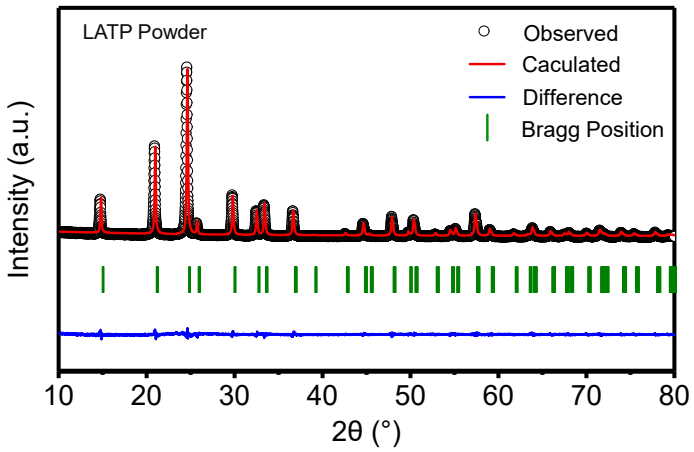

Fig. S10 Rietveld refined XRD pattern of LATP powder.

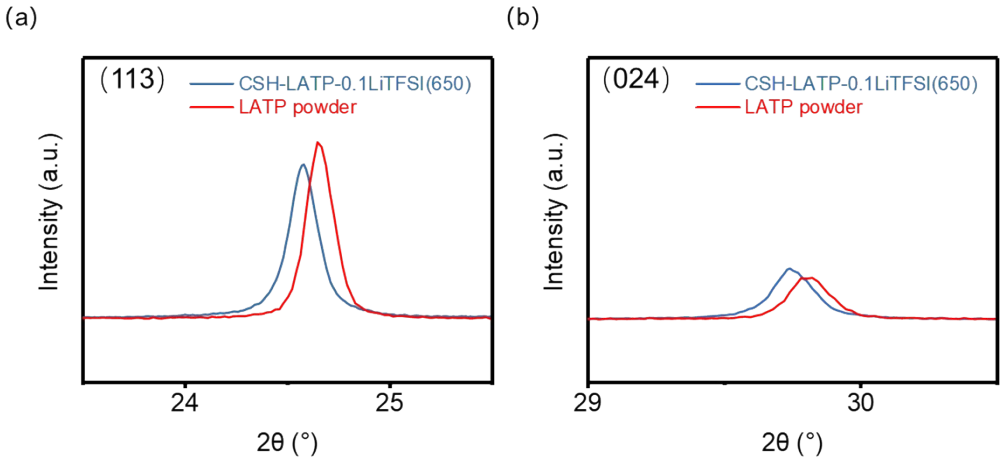

Fig. S11 Enlarged views of (a) (113) and (b) (024) diffraction peaks.

Table S1 The hardness test results of LATP pellets at different experiment condition

Sample	Temperature of cold sintering	H-IT/GPa	HV	E-IT/GPa
CSH-LATP(650)	130	0.357	33.0	36.18
CSH-LATP-0.1LiTFSI(650)	130	2.286	211.8	80.17
CSH-LATP-0.1LiTFSI(650)	200	5.041	466.9	114.72
H-LATP(900)	/	5.133	475.4	115.00

Table S2 Rietveld fitting results of LATP and CSH-LATP-0.1LiTFSI(650) electrolyte samples.

Sample	space group	a=b（Å）	c（Å）	α=β（°）	γ（°）	V（Å^3）	R_w
LATP	R-3C	8.49916	20.79765	90	120	1301.059	7.64
CSH-LATP-0.1LiTFSI	R-3C	8.49101	20.89296	90	120	1304.517	11.7

Table S3 Crystallographic data of LATP and CSH-LATP-0.1LiTFSI(650) electrolyte samples.

Sample	Atom	Site	x	y	z	Occupancy
LATP	Li	6b	0	0	0	1.1277
	Al	12c	0	0	0.14128	0.15
	Ti	12c	0	0	0.14128	0.8126
	P	18e	0.28952	0	0.25	1
	O1	36f	0.18539	0.98977	0.19037	1
	O2	36f	0.18245	0.15861	0.08133	1
CSH-LATP-0.1LiTFSI(650)	Li	6b	0	0	0	1.2691
	Al	12c	0	0	0.14131	0.15
	Ti	12c	0	0	0.14131	0.8362
	P	18e	0.28830	0	0.25	1
	O1	36f	0.18231	0.99103	0.18898	1
	O2	36f	0.18750	0.16430	0.08169	1

Table S4 Comparison of the electrochemical performance using Li anode and $LiFePO_4$ cathdoe and relative density and ionic conductivity of CSH-LATP-0.1LiTFSI(650) with other reported works.

Ref.	Ionic conductivity at RT (S cm^{-1})	Sintering parameters	Initial discharge capacity (mAh g^{-1})	Capacity decay rate per cycle
[1]	8.73×10^{-4}	900°C-6h	149.7	5.19% at 1C
[2]	4.74×10^{-4}	900°C-12h	157.6	4.92% at 0.1C
[3]	1.15×10^{-4}	/	154.7	5.75% at 0.2C
[4]	6.46×10^{-4}	/	139.72	7.24% at 0.5C
[5]	/	800°C-6h	130.1	4.8% at 0.5C
[6]	1.06×10^{-3}	/	164	6.83% at 0.2C
[7]	/	900°C-10h	166.3	10.32% at 0.4C
[8]	1.13×10^{-4}	800°C-2h	119.4	9.5% at 0.5C
This work: CSH-LATP-0.1LiTFSI(650)	7.85×10^{-4}	650°C -2h	149.7	4.17% at 0.5C

References

1. Huang, C.; Huang, S.; Wang, A.; Liu, Z.; Pei, D.; Hong, J.; Hou, S.; Vitos, L. and Jin, H. *J. Mater. Chem. A*, **2022**, *10*, 25500.
2. Wang, Y.; Wang, L.; Shi, Q.; Zhong, C.; Gong, D.; Wang, X.; Zhan, C. and Liu, G. *J. Energy Chem.* **2023**, *80*, 89-98.
3. Rong, Y.; Lu, Z.; Jin, C.; Xu, Y.; Peng, L.; Shi, R.; Gu, T.; Lu, C. and Yang, R. *ACS Sustainable Chem. Eng.* **2023**, *11*, 785-795.
4. Kibret, D.; Mengesha, T.; Walle, K.; Wu, Y.; Chang, J.; Jose, R. and Yang, C. *J. Energy Storage* **2024**, *94*, 112523.
5. Luo, L.; Zheng, F.; Gao, H.; Lan, C.; Sun, Z.; Huang, W.; Han, X.; Zhang, Z.; Su, P.; Wang, P.; Guo, S.; Lin, G.; Xu, J.; Wang, J.; Li, J.; Li, C.; Zhang, Q.; Wu, S.; Wang, M. and Chen, S. *Nano Res.* **2023**, *16(1)*: 1634-1641.
6. Cho, Y.; Mong, A.; Hoang, H. and Kim, D. *J. Energy Storage* **2024**, *92*, 112295.
7. Lei, M.; Fan, S.; Yu, Y.; Hu, J.; Chen, K.; Gu, Y.; Wu, C.; Zhang, Y. and Li, C. *Energy Storage Mater.* **2022**, *47*, 551-560.
8. Tran, H.; Wu, Y.; Chien, W.; Wu, S.; Jose, R.; Lue, S. and Yang, C. *ACS Appl. Energy Mater.* **2020**, *3*, 11024-11035.